

WP4

Forecast numerical modelling for coastal extreme weather and flooding risk management

Activity 4.2

Hydrological model downscaling for coastal flooding forecast and prevention

D4.2.1

Hydrological model adaptation for coastal flooding forecast prevention

PROJECT AND ACTIVITY DETAILS

Project Acronym	AdriaMORE
Project title	Adriatic DSS exploitation for MONitoring and Risk management of coastal Extreme weather and flooding
Funding Line	Priority Axis 2, Specific Objective 2.2
Project Partners	LP Abruzzo Region (Italy) P1 Dubrovnik and Neretva Region (Croatia) P2 Meteorological and hydrological service (Croatia) P3 National Research Council (Italy)
Starting date	January 1, 2018
Activity number	4.2
Activity Title	Hydrological model downscaling for coastal flooding forecast prevention
Work Package	WP4: Forecast numerical modelling for coastal extreme weather and flooding risk management
Activity Summary	Activity 4.2, within work package 4, is devoted to the implementation of the hydrological model CHyM with a new calculation scheme that takes into account the storm surge forcing in coastal floods.
Deliverable number	4.2.1
Deliverable Summary	This deliverable is aimed at describing the implemented parameterization for the storm surge in the river mouth of Neretva and Pescara rivers.
Main Author	Valentina Colaiuda, valentina.colaiuda@univaq.it
Main Author's organization	CETEMPS
Other Author's	Annalina Lombardi, Barbara Tomassetti, Kreso Pandzic
Data of issue	April, 30 2019
Total Number of pages	34
Distribution list	Italy-Croatia CBC Programme, AdriaMORE partners

This document has been produced with the contribution of the EU co-financing and the Interreg Italy-Croatia CBC Programme. The content reflects the author's views; the Programme authorities are not liable for any use that may be made of the information contained therein.

Table of contents

<u>Introduction</u>	Pag. 4
<u>1. The CETEMPS Hydrological model (CHyM)</u>	Pag. 5
1.1 Spatialization algorithms	Pag. 5
1.2 Surface runoff	Pag. 6
1.3 Evapotranspiration	Pag. 7
1.4 Melting	Pag. 8
1.5 Infiltration	Pag. 9
1.6 Return flow	Pag. 9
1.7 Hydrological stress index BDD	Pag. 9
<u>2. The parameterization of stream flow-sea interaction</u>	Pag. 11
2.1 Bibliographic background	Pag. 11
2.2 The “waveheight” module	Pag. 12
<u>3. Pescara river</u>	Pag. 16
3.1 Case study 24 th December 2010	Pag. 16
3.2 Case study 15 th November 2010	Pag. 19
3.3 Case study 28 th November 2018	Pag. 24
<u>4. Neretva river</u>	Pag. 28
4.1 Case study 1 st – 3 rd December 2010	Pag. 28
<u>References</u>	Pag. 33

Introduction

In order to overcome to the objective foreseen for Deliverable 4.2.1, the CETEMPS Hydrological Model (CHyM, hereafter) has been updated to a new version (v. 5.040), containing the calculation scheme to simulate the barrier effect of the sea in case of storm surge. The implemented parameterization is inspired to the scientific literature and other approaches usually found in the U.S., but is adapted and calibrated over the target basins on a case study-basis. The present document is organized as follows:

Paragraph 1: contains the physical concept beyond the CHyM model and the main equation used to simulate the hydrological cycle;

Paragraph 2: is dedicated to the detailed description of the storm surge parameterization in terms of numerical approach and workflow within the CHyM code;

Paragraph 3: is devoted to the calibration in the Pescara river mouth. The hydro-meteorological description, available observations and simulation results are given;

Paragraph 4: is devoted to the calibration in the Neretva river mouth. The hydro-meteorological description, available observations and simulation results are given.

1. The Cetemps Hydrological Model (CHyM)

CHyM model is a grid-distributed, physical-based hydrological model. All the relevant physical quantity are defined on an equally-spaced grid. The model can be used to simulate the hydrological cycle in any geographical domain with any spatial resolution up to the resolution of implemented Digital Terrain Model (DTM), namely 270 m for the Pescara and Neretva basins (fig. 1.1).

As a complete description of the model goes beyond the aim of this deliverable, only the main features of the model will be given in the following sections. For a complete description of CHyM, please, refer to Sohoroshan et al. (2008), as well as Tomassetti et. al. (2005) and Verdecchia et al. (2008) for its operational activities.

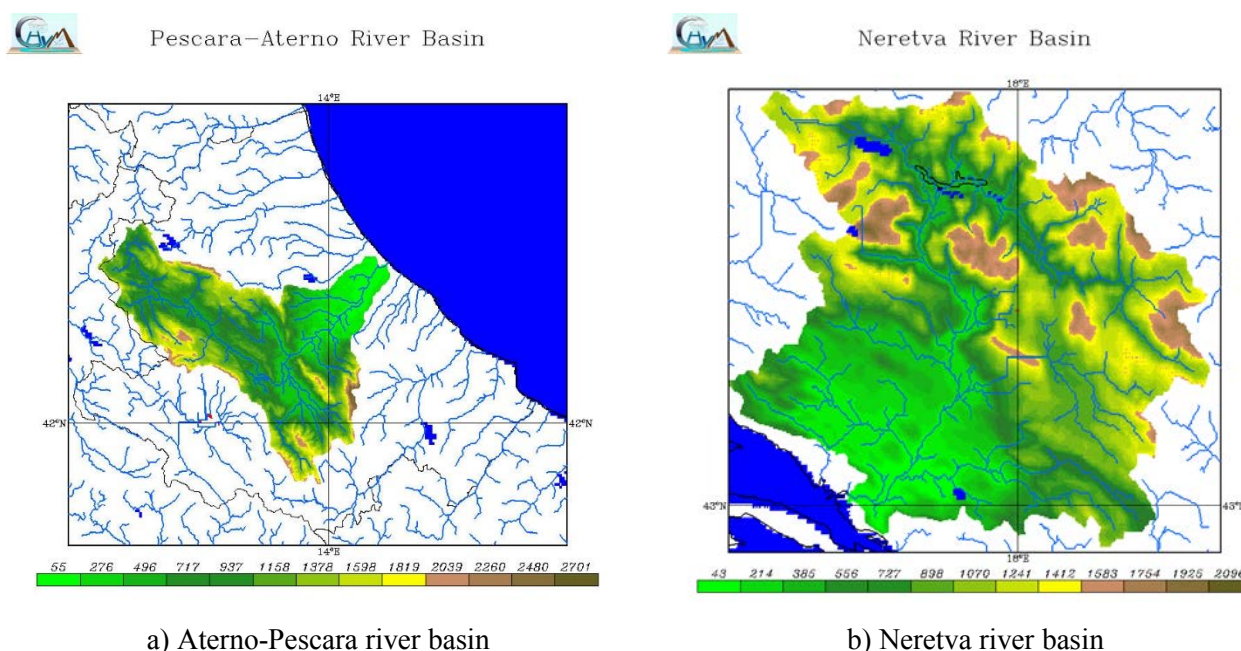


Figure 1.1: target catchments altitudes (m a.s.l. - shaded colours) and their drainage network (blue lines) as rebuilt by the cellular automata techniques used in the CHyM model.

1.1 Spatialization algorithms

CHyM model implements an original and sophisticated technique to correct the DTM singularities in order to correctly rebuilt a drainage network where the correct flow direction is associated to each grid-point. The algorithm is based on the main concept of Cellular Automata (CA hereafter) theory (Packard and Wolfram 1985). A complete description of CA based approach to smooth DTM is reported in Coppola et al. (2007) and can be quickly resumed as following:

- CHyM grid is considered an aggregate of cellular automata;
- The status of a cell corresponds to the value of a CHyM field (DTM, in this case);

- The state of the cells in the lattice is updated according to a local rule; this rule establish that the DTM value of the central cell is smoothed according to the average value of the surrounding cells;
- All the cells of the lattice are updated synchronously;
- Update ends when the flow direction can be established for all the cells.
- It has been shown (Coppola et al. (2007)) that the proposed numerical technique allows to realistically rebuild the drainage network for many basins of the world simulated with different resolutions. The proposed algorithm also allow to significantly reduce the correction of the DTM array, the whole process can be resumed in 3 steps:
- The original DTM is used for establishing the flow direction except for the grid points where singularities occur;
- The whole DTM is then smoothed using the CA based numerical technique until all the singularities are solved and the whole stream flow network is established;
- Once the flow direction is established for each cell, the original DTM is used and only the height of those cells draining toward a cell with greater elevation is modified.

CA smoothing techniques are also used to ingest different and heterogeneous meteorological dataset (observed, estimated or simulated) to rebuild the precipitation and temperature fields. The basic is to consider that the rainfall at a given grid point is given by the weighted average of the precipitation in the surrounding cells, with the weights depending on the distances between the grid points where a precipitation data is present. As shown in Coppola et al. (2007) the iteration of this CA based algorithm allows to obtain a reconstruction of complex precipitation pattern resulting more realistic with respect to the one obtained with a simple geometrical interpolations.

1.2 Surface Runoff

As for many other hydrological models (for a general reference see, as an example, Singh and Frevert, 2002, surface routing is calculated according to the kinematic wave approximation of the shallow water (Lighthill and Whitam, 1955). The equations used by CHYM model to simulate the surface routing overland and the channel flow are the continuity and momentum conservation equations:

$$\frac{\partial A}{\partial t} + \frac{\partial Q}{\partial t} = q \quad [1.2.1]$$

$$Q = \alpha A^m \quad [1.2.2]$$

where A is the flow cross-sectional area, Q is the flow rate of water discharge, q is the rate of lateral inflow per unit of length due to all the physical processes contributing the hydrological cycle, t is

the time, α is the kinematic wave parameter, and m the kinematic wave exponent usually assumed as 1. The kinematic wave parameter α has the dimension of a speed and can be written as:

$$\alpha = \frac{\sqrt[2]{S^3 \sqrt{R^2}}}{M_{lu}} \quad [1.2.3]$$

where S the longitudinal bed slope of the flow element, M_{lu} is the Manning's roughness coefficient depending on the land use type μ and R is the hydraulic radius that can be calculated as a linear function of the drained area D according to:

$$R = \beta + \gamma D^\delta \quad [1.2.4]$$

where β , γ and δ are empirical constants to tune with during the calibration. The quantity D represents the area in the upstream of the flow element; in other words, with the previous equation, we assume that the cross section of a flow channel, in a generic point, can be calculated as a linear function of upstream area (the exponent δ is usually very close to 1)

1.3 Evapotranspiration

The potential evapotranspiration is computed as a function of the reference evapotranspiration that is the evapotranspiration in soil saturation condition (Thornthwaite and Mather, 1957):

$$ET_p = k_c ET_0 \quad [1.3.1]$$

where k_c is the crop factor that is a function of crop type. The reference evapotranspiration ET_0 is a linear function of temperature and is calculated according to the following formula:

$$ET_0 = \alpha + \beta NW_{ta}(h, T)T \quad [1.3.2]$$

where N is daily maximum sunshine hours, $W_{ta}(h, T)$ is the compensation factor depending on the elevation h and temperature T . The coefficients α and β are to be estimated and this is carried out fitting with the least squared method the Thornthwaite formula, namely:

$$16 \frac{n(m)}{30} \frac{N(m)}{12} \left[10 \frac{T(m)}{K_1} \right]^{K_2} = \alpha + \beta NW_{ta}(h, T)T \quad [1.3.3]$$

where $n(m)$ is the number of days of month m , N is the daily maximum sunshine hours for the month m , $T(m)$ is the monthly average temperature, k_1 and k_2 are the thermal indexes.

The compensation factor $W_{ia}(h, T)$ is a function of elevation and temperature and is calculated from:

$$W_{ia}(h, T) = A(h)T^2 + B(h)T + C(h) \quad [1.3.4]$$

The coefficient $A(h)$, $B(h)$ and $C(h)$ have been estimated for different range of elevation according to the table reported by Dorembos et al. (1984).

The actual evapotranspiration ETA is indeed a fraction of potential evapotranspiration ET_p and it is calculated as a linear function of ground relative humidity GRH, more specifically ETA is zero in arid condition ($G_{RH} < 0.2$) and it is equal to ET_p for $G_{RH} > 0.7$. For other values of ground humidity, the evapotranspiration term is calculated as a linear function of G_{RH} :

$$ETA = \frac{G_{RH} - 0.2}{0.7 - 0.2} ET_p = \frac{G_{RH}}{0.7 - 0.2} K_c ET_0 \quad [1.3.5]$$

For other details about the estimation of the evapotranspiration term refer to Todini (1996) and Thornthwaite and Mather (1955).

1.4 Melting

CHyM model implements a temperature-index melt parameterization based on the assumption that melt

rates is given by the sum of two terms. The first is linearly related to the air temperature, which is regarded as an integrated index of the total energy available for melt, while the second term is proportional to the incoming net solar radiation. Within this approach, melting is assumed to occur when the temperature T is above a threshold level T_T (typically 1°C). In fact it has been recognized (Pellicciotti et al., 2005) that this approach reproduce in a realistic way the observed melting rate in the Alpine region. The melting rate M (mm of equivalent precipitation per hour) is calculated as following:

$$M = T_F T + S_{RF} (1 - \alpha) G_{\downarrow} \quad [1.4.1]$$

The factor of proportionality for the first term T_F is the so called “temperature factor” (typical value around $0.05 \text{ mm}/^\circ\text{C}$), the coefficient S_{RF} is the shortwave radiation factor, and its typical value is around $0.0094 \text{ mm/h M}^2/(\text{Watt } ^\circ\text{C})$, α is the fraction of solar radiation reflected by the surface, T is the ground temperature estimated by CHyM model. In the previous formula G_{\downarrow} is the incoming short wave solar radiation estimated as follows:

$$G_{\downarrow} = C_s A_{tr} \sin \Psi \quad [1.4.2]$$

where C_s is the solar constant (1368 Watt/m^2) and A_{tr} is the net sky transmissivity (Stull, 1999).

1.5 Infiltration

The infiltration process is modelled using a conceptual model similar to those proposed by several authors as Overton (1964), Singh and Yu (1990). Within this approach, we schematize the soil as two reservoirs of water: the precipitation infiltrates in the upper soil layer until the saturation level is reached. The water of the first reservoir (upper layer) also infiltrate (percolation) toward the lower soil layer. The total amount of water that infiltrates I is also saved at each time step in order to evaluate the return flow (see below).

1.6 Return flow

Return flow is parameterized assuming that the contribute to each elementary channel-cell is proportional to the total infiltration in the upstream basin in the last N months:

$$R_f = \int_{Up} ds \int I(t, s) dt \quad [1.6.1]$$

the infiltration term I described in the previous paragraph is integrated over the whole upstream basin of each cell and the time integral is carried out over the last N months being N a value to be optimized during the calibration process. In practice, we assume that infiltrated water contributes to the return flow within the same catchment. The return flow is then calculated, for each cell, as a linear function of R_f term, and the linear coefficient is optimized during the calibration phase with typical values around $5 \times 10^{-7} \text{ mm hour}^{-1} \text{ Km}^{-2}$.

1.7 Hydrological stress index BDD

Flood forecast is a challenge in hydrological modelling, as there are still many issues related to flood detection and observation. As mentioned in the previous section, a hydrological model is able to calculate the natural river discharge over each grid-point of the drainage network. However, direct methods for the discharge measurements does not exist, corrected in the strictest sense of the word, as this physical quantity is estimated through the use of indirect methods (e.g. rating curves). Those methods are based on the hydrometric level measurements and need to be re-calibrated according systematically, especially after flood events that alters the river bed condition and the wet area significantly. Moreover, as the hydrological warning state is assigned by the Civil Protection Agencies according to pre-defined water level thresholds, it is not trivial to establish a correspondence with the discharge value, when rating curves are not updated. Another important issue in using hydrometric threshold is related to the spatial representativeness of such information, which is given at station level, excluding all other un-instrumented river segments. For this reason, a hydrological stress index has been developed in order to identify river segments at flood risk. The BDD (Best Discharge-Based) index has been developed to this aim, by relating the natural discharge computed in the CHyM model calculation scheme with the wet area, calculated as a function of the drained area upstream:

$$BDD_i(t_1 - t_2) = \frac{\max_{t_1 \rightarrow t_2} (Q_i(t))}{R_i^2} \quad [1.7.1]$$

where:

- Q is the discharge of the grid-point i ;
- R the hydraulic radius, calculated as a function of the drained area;
- t is the considered time interval (typically, $t_1 - t_2 = 24$ hours).

To this end, hydrological stress occurs when the river section is not able to “contain” a certain quantity of water. Different hydrological stress degrees are assigned to BDD values though the definition of two index threshold, to which color-codes are assigned, accordingly to the Civil Protection warning level defined in table 1.7.1. The aforementioned thresholds have been calibrated and statistically evaluated in Lombardi et al. (2019).

Chosen BDD thresholds are 6 mm/h for pre-alert warning level (orange threshold) and 12 mm/h for alert warning level (red threshold)

Table 1.7.1: civil protection warning level corresponding to hydrometric thresholds and associated BDD thresholds

Colour-code warning level	Warning level	Hydrological status description	BDD associated value
	Below THR 1	No flood. Regular hydrometric levels	Not defined
	Above THR1	Flow peak with limited erosion and transport. Hydrometric levels corresponds to the floodplain and river expansion to the levee. The natural floodplain is exceeded	$BDD < 6$ mm/h
	Above THR2	Flow peak with limited erosion and transport. Hydrometric levels corresponds to the floodplain and river expansion to the levee. The natural floodplain is exceeded.	$6 \leq BDD < 12$ mm/h
	Above THR3	Significant discharge peak and diffused erosion and transport. Hydrometric levels corresponds to the whole riverbed.	$BDD \geq 12$ mm/h

2. The parameterization of stream flow-sea interaction

In order to simulate the friction due to stream flow-sea interaction, a new parameterization has been added in the CHyM workflow, written in a new module called “*waveheight*”. In this module, the measured (or simulated) sea level at the river mouth grid-point is assimilated, in order to give a Manning’s coefficient correction to increment the friction and reduce the flow velocity at the estuary.

2.1 Bibliographic background

In order to modify the estuary dynamics of the river flow into the hydrological model, a bibliographical investigation has been carried out in a first phase, in order to identify the most suitable method to introduce the sea level measurement to be combined with the runoff calculation. According to Garzon and Ferreira (2016), a first approach consists in modifying the Manning’s coefficient at the river mouth grid point, accordingly to the obstruction degree. In the CHyM model, the Manning’s coefficient values are fixed for each type of land use coverage and slope (see formula 1.2.3), and inferred from the scientific literature. As described in the previous paragraph 1.2, this coefficient is involved in the surface runoff calculation. Each fixed value is then corrected according to the following formulas, depending on the upstream drained areas (*drai*). In particular, for drained areas higher than 100 km² (*thr*), M_{lu} is lowered by dividing it for an empirical, dimensionless parameter δ (< 1), while smallest drained areas are computed according to formula [2.1.1].

- for $drai > thr$ (100 m², threshold that discriminates river grid cells)

$$n = \frac{M_{lu}}{\delta} \quad [2.1.1]$$

- for $drai < thr$

$$n = \frac{M_{lu}}{(1 + \delta - 1) \cdot \frac{(1 + drai - thr)}{thr}} \quad [2.1.2]$$

The physical interpretation of such correction is that the Manning’s coefficient, which is connected to the friction of the water flow over the soil slope, is reduced when the flow is consistent and decreases toward the river outlet.

As the river mouth is obstructed by the upstream sea motion, under particular meteorological conditions, the river channel may have higher friction values that needs to be considered. For this purpose, a fixed value of M_{lu} is not sufficient, as the coefficient should be varied according to the sea obstruction degree.

According to a recent study from Garzon and Ferreira (2016), where a hydrodynamic model has been used to reproduce the hydrometric profile of the Potomac and James rivers, the modification of the river outlet Manning’s coefficient can be accomplished through sensitivity tests, made by introducing a range of correction coefficients (Cowan, 1976 and Passeri, 2011). Values of such correction coefficients are chosen in order to minimize the distance between simulated and observed hydrometric levels.

The described method can be partially applied on the AdriaMORE target basins, as no hydrometric sensor are installed in the last segment of the Pescara river (the last one is located 6 km upstream) and no rating curve are available for Neretva hydrometers, as well. Nevertheless, the use of a hydrological stress index in place of river discharge, requires a different kind of calibration, which is based on simulating the correct warning level, rather than the correct discharge values. For this reason, the river discharge computation, which depends on the Manning's coefficient, according to the description given in the previous section, act as a vehicle to tune the warning level.

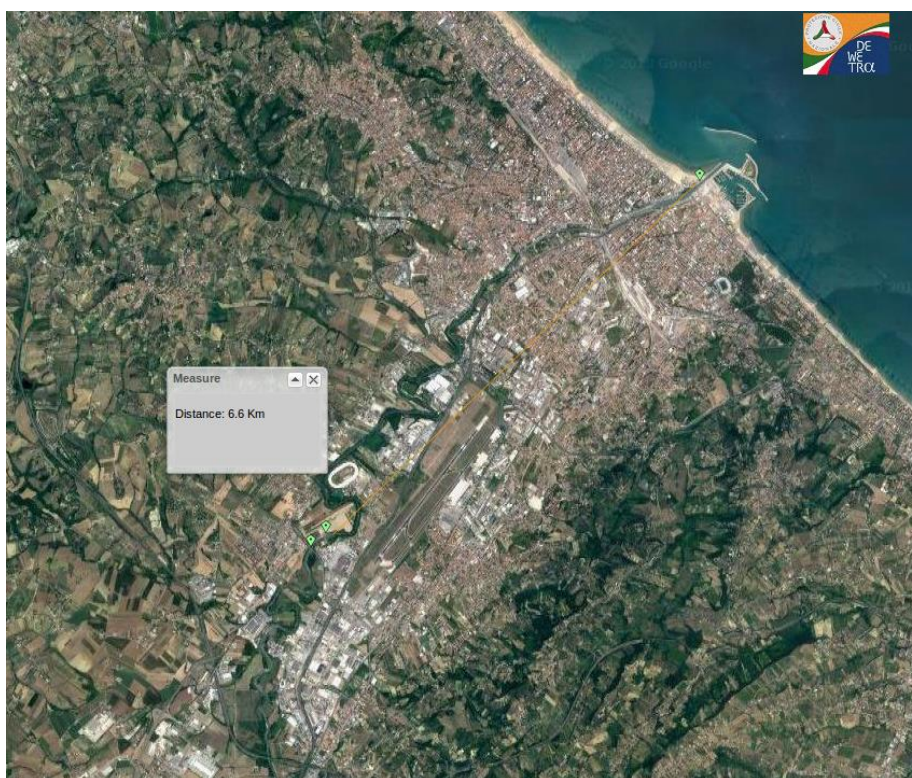


Figure 2.1.1: hydrometric sensors spatial distribution along the Pescara river (green pinpoints). The last hydromter is located at 6.6 km before the river mouth. The pinpoint positioned close to the Pescara harbour is used the sea –level sensor

2.2 The “waveheight” module

The *waveheight* module contains physical parameterizations able to modify the Manning's coefficient as to increment the friction at the river outlet, when the sea level reaches critical values. The module is called within a hieratically upper module (*chymintegr*) where all dynamical fields are calculated (fig. 2.2.1)

```

valentina@pcvcolaiuda: ~
call runoffspeed(0.0)
call plotting
call writeintes
time=mchym(4) ; call gmafromm5index(time,hour,day,month,year)
write(6,'(12x,a)') 'Start of integration. Hereafter output is '//
2 'sent to chymlog file'
call getlun(logun(2)) ; call mvsetflags('CHyM log unit',float(logun(2)))
open(logun(2),file='chymlog',status='unknown')
hourstep=0
return
end

subroutine chymintegr(nstep)
use chyndata , only : mchym,time,hour,day,month,year,now,hourstep
use chyndata , only : srcflag
implicit none
integer increasetime,idhour,indexofyear,nstep
do idhour=1,nstep
hourstep=hourstep+1
call writeoutfile(0)
call waveheight
call temperature
call rainfall
call snowcover
time=increasetime(time)
call gmafromm5index(time,hour,day,month,year)
call dataorafromday (hour,day,month,year,now)
call writeoutfile(1)
call snowacc
call evapotranspiration
call melting
call groundwater
call writeoutfile(2)
call returnflow
call runoff
call writeoutfile(3)
end do
return
end

subroutine chymciao
use chyndata , only : logun,sstr1
implicit none
integer i,lenstr
write(6,'(12x,a)') 'Done.' ; call writestatus('End of run')
sstr1= 'Closing chym login unit '
do i=1,10
-- INSERT --

```

Figure 2.2.1: call to the “waveheight” modul within the CHyM code.

The subroutine sequence starts with the activation of the *subroutine runoffspeed*, which makes the runoff velocity a dynamic field over the grid-points close to the river outlet, depending on the sea level at the river mouth. In the oldest version of the model, the subroutine was called once at the beginning of the simulation; in the updated version, the subroutine is called at each hourly time step. In the first iteration, the river mouth and its 8 upstream grid-cells are identified: the Manning’s coefficient will be corrected only in these points (fig. 2.2.2). The original CHyM Manning’s coefficient n (see [2.1.1] and [2.1.3]) is changed according to the corrective coefficient c , as expressed in the following formula:

$$n = n + \frac{c}{k + 1} \quad [2.2.1]$$

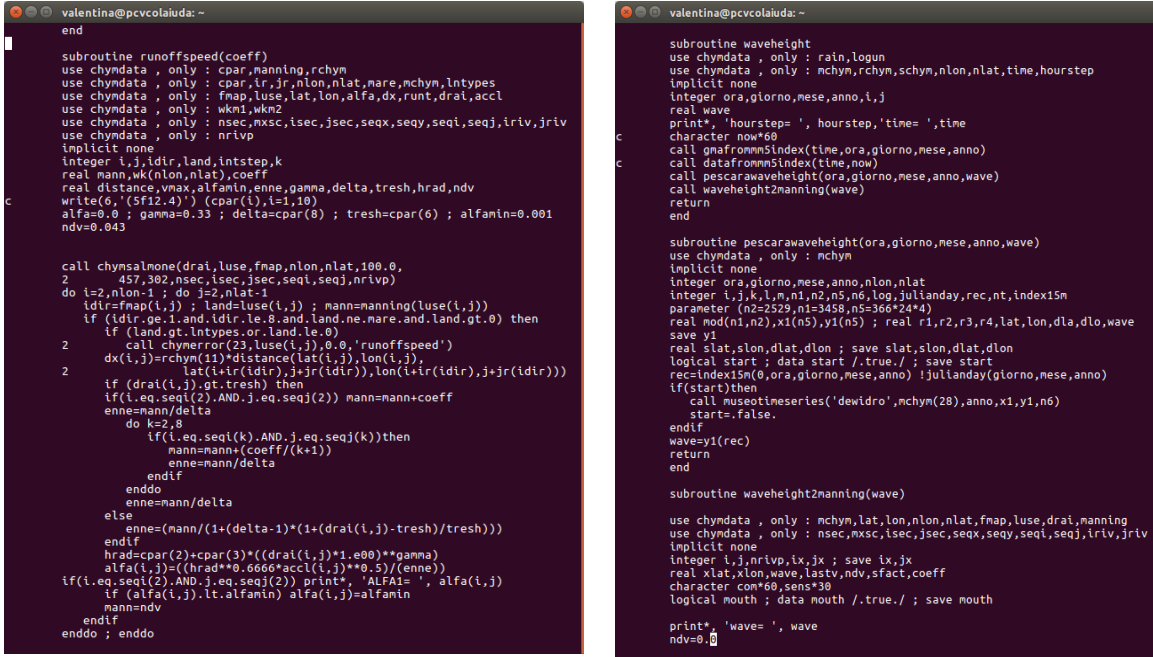
Where $1 \leq k \leq 8$ is the grid-point index that identifies the 8 river cells before the river mouth.

Two distinct operations are included in the *waveheight* module:

1. sea level data (h_{sea}) are read in input in the embedded *subroutine waveheight* (sources are “Pescara Porto” station for the Pescara river and “Ploce” station for the Neretva river);

- a different and calibrated value of c is associated to each h_{sea} bin, taking into account different obstruction degree being caused by different sea level conditions. c values are calibrated in the case studies presented in the following sections 3 and 4, considering the recommendations suggested by the USGS manual FHWA-TS-84-2014 (fig. 2.2.3).

Sea level bins have been divided through a historical analysis of the Pescara Porto station timeseries.



```

valentina@pcvcolaiuda: ~
end

subroutine runoffspeed(coeff)
use chynndata , only : cpar,manning,rchym
use chynndata , only : cpar,ir,jr,nlon,nlat,mare,mchym,lntypes
use chynndata , only : fnap,luse,lat,lon,alfa,dx,runt,drai,accl
use chynndata , only : wkn1,wkn2
use chynndata , only : nsec,mxsc,isec,jsec,seqx,seqy,seql,seqj,iriv,jriv
use chynndata , only : nrivp
implicit none
integer i,j,idir,land,intstep,k
real mann,wk(nlon,nlat),coeff
real distance,vmax,alfamin,enne,gamma,delta,tresh,hrad,ndv
write(6, '(5f12.4)') (cpar(i),i=1,10)
alfa=0.0 ; gamma=0.33 ; delta=cpar(8) ; tresh=cpar(6) ; alfamin=0.001
ndv=0.043

call chynsalnone(drai,luse,fnap,nlon,nlat,100.0,
2 457,302,nsec,isec,jsec,seqj,seqj,nrivp)
do i=2,nlon-1 ; do j=2,nlat-1
idir=fnap(i,j) ; land=luse(i,j) ; mann=manning(luse(i,j))
if (idir.ge.1.and.idir.le.8.and.land.ne.mare.and.land.gt.0) then
if (land.gt.lntypes.or.land.le.0)
2 call chymerror(23,luse(i,j),0.0,'runoffspeed')
dx(i,j)=rchym(11)*distance(lat(i,j),lon(i,j),
2 lat(i+idir),j+jr(idir)),lon(i+idir),j+jr(idir))
if (drai(i,j).gt.tresh) then
if(i.eq.seqj(2).AND.j.eq.seqj(2)) mann=mann+coeff
enne=mann/delta
do k=2,8
if(i.eq.seqj(k).AND.j.eq.seqj(k))then
mann=mann+(coeff/(k+1))
enne=mann/delta
endif
enddo
enne=mann/delta
else
enne=(mann/(1+(delta-1)*(1+(drai(i,j)-tresh)/tresh)))
endif
hrad=cpar(2)+cpar(3)*((drai(i,j)+1.e00)**gamma)
alfa(i,j)=((hrad**0.0606**accl(i,j)**0.5)/(enne))
if(i.eq.seqj(2).AND.j.eq.seqj(2)) print*, 'ALFAi= ', alfa(i,j)
if (alfa(i,j).lt.alfamin) alfa(i,j)=alfamin
mann=ndv
endif
enddo ; enddo
end

subroutine waveheight
use chynndata , only : rain,logun
use chynndata , only : mchym,rchym,schym,nlon,nlat,time,hourstep
implicit none
integer ora,giorno,mese,anno,i,j
real wave
print*, 'hourstep= ', hourstep,'time= ',time
character now*60
call gnafromm5index(time,ora,giorno,mese,anno)
call datafromm5index(time,now)
call pescarawaveheight(ora,giorno,mese,anno,wave)
call waveheight2manning(wave)
return
end

subroutine pescarawaveheight(ora,giorno,mese,anno,wave)
use chynndata , only : mchym(ora,giorno,mese,anno,wave)
implicit none
integer ora,giorno,mese,anno,nlon,nlat
integer i,j,k,l,m,n1,n2,n5,n6,log,julian,rec,nt,index15m
parameter (n2=2529,n1=3458,n5=366*24*4)
real mod(n1,n2),x1(n5),y1(n5) ; real r1,r2,r3,r4,lat,lon,dla,dlo,wave
save y1
real slat,slon,dlat,dlon ; save slat,slon,dlat,dlon
logical start ; data start /.true./ ; save start
rec=index15m(0,ora,giorno,mese,anno) !jullanday(giorno,mese,anno)
if(start)then
call museotimeseries('dewidro',mchym(28),anno,x1,y1,n6)
start=.false.
endif
wave=y1(rec)
return
end

subroutine waveheight2manning(wave)
use chynndata , only : mchym,lat,lon,nlon,nlat,fnap,luse,drai,manning
use chynndata , only : nsec,mxsc,isec,jsec,seqx,seqy,seql,seqj,iriv,jriv
implicit none
integer i,j,nrivp,ix,jx ; save ix,jx
real xlat,xlon,wave,lastv,ndv,sfact,coeff
character con*60,sens*30
logical mouth ; data mouth /.true./ ; save mouth

print*, 'wave= ', wave
ndv=0.0

```

a) In the «waveheight» module an adjustment coefficient corrects the Manning's coefficients and, thus, the alpha calculation on [1.2.3]

b) In the «waveheight» the adjustment coefficients is assigned by considering the sea level data from the Pescara harbour station

Figure 2.2.2: organization of the *waveheight* module within the CHyM fortran code

Table 2.--Factors that effect roughness of the channel--Continued

Channel conditions	n value adjustment ^{1/}	Example
Effect of obstruction (n ₃)	Negligible	0.000-0.004 A few scattered obstructions, which include debris deposits, stumps, exposed roots, logs, piers, or isolated boulders, that occupy less than 5 percent of the cross-sectional area.
	Minor	0.005-0.015 Obstructions occupy less than 15 percent of the cross-sectional area and the spacing between obstructions is such that the sphere of influence around one obstruction does not extend to the sphere of influence around another obstruction. Smaller adjustments are used for curved smooth-surfaced objects than are used for sharp-edged angular objects.
	Appreciable	0.020-0.030 Obstructions occupy from 15 to 50 percent of the cross-sectional area or the space between obstructions is small enough to cause the effects of several obstructions to be additive, thereby blocking an equivalent part of a cross section.
	Severe	0.040-0.050 Obstructions occupy more than 50 percent of the cross-sectional area or the space between obstructions is small enough to cause turbulence across most of the cross section.
Amount of vegetation (n ₄)	Small	0.002-0.010 Dense growths of flexible turf grass, such as Bermuda, or weeds growing where the average depth of flow is at least two times the height of the vegetation; supple tree seedlings such as willow, cottonwood, arrowweed, or saltcedar growing where the average depth of flow is at least three times the height of the vegetation.

Figure 2.2.3: correction coefficient values recommended by USGS and related to the channel obstruction conditions (from: “*Guide for selecting Manning’s roughness coefficients for natural channels and flood plains*”, April 1984)

3. Pescara river

Three case studies with different hydro-meteorological forcings have been chosen for the Abruzzo region, in order to calibrate the correction coefficient, described in the previous section, and test the performance of the new CHyM model version for coastal flooding early-warning. The three chosen case studies and their characteristics are summarized in table 3.1

Table 3.1: Pescara river case study summary

Case study date	Hydro-meteorological forcings24 de
24 th December 2010	No rainfall occurrence, storm surge only
17 th November 2017	Heavy rainfall and storm surge
28 th November 2018	Moderate rainfall and storm surge

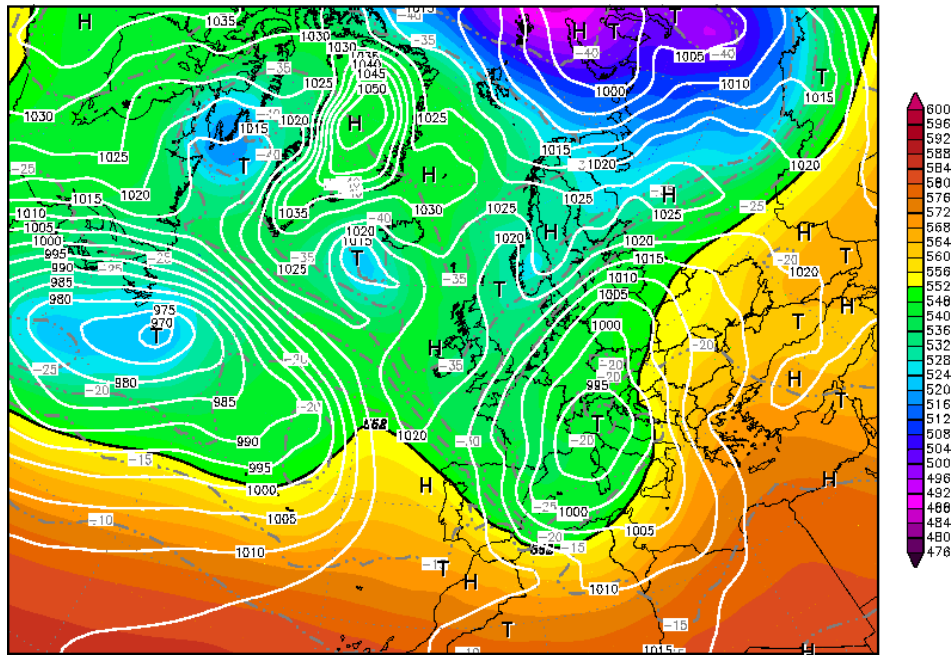
3.1 Case study 24th December 2010

This first case study has been chosen in collaboration with the Functional Centre of Abruzzo Region. This is a particular important case study, as the Pescara river level rose up in the canal port area, without heavy rain occurrence. The pre-alert warning level was issued by the local civil protection authorities, as a consequence of citizens warnings.

Synoptic description

A deep through is extending from the North Atlantic Ocean toward the central Mediterranean area. A barometric pressure minimum at ground level is located over the northern part of the Adriatic sea, rapidly moving in South-East direction (fig. 3.1.1). Cold air from Northwest is flowing along the Adriatic regions of Italy (fig. 3.1.2).

Init : Fri,24DEC2010 00Z Valid: Fri,24DEC2010 00Z
 500 hPa Geopot.(gpm), T (C) und Bodendr. (hPa)



Daten: GFS-Modell des amerikanischen Wetterdienstes
 (C) Wetterzentrale
 www.wetterzentrale.de

Figure 3.1.1: 500 hPa geopotential height over Europe on 25th Dec 00UTC (colour shades) and pressure at ground level (isolines).

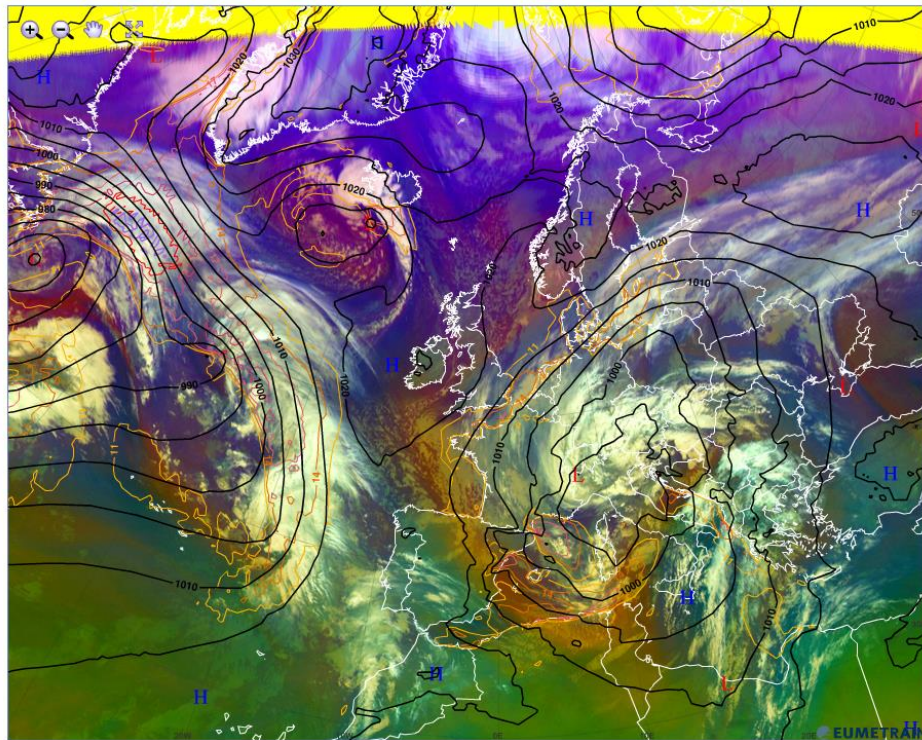


Figure 3.1.2: Airmass RGB satellite image (Eumetrain©) over Europe on 24th December 2010 06UTC. Black isolines represents atmospheric pressure at ground level.

In figure 3.1.3 the sea level timeseries observed at the “Pescara Porto” station during the event is reported. The sea level increased on 24th December early morning. Citizens’ warning about the increasing river level, received by the Abruzzo Region Functional Centre, were given by people living around the canal port during the morning of the same day. Clear sky conditions were present and no evidence of precipitation was found over the wall catchments days before; low precipitation amount (10-15 mm/24h) affects the southern area of the region, outside the basin boundaries. (fig. 3.1.4).

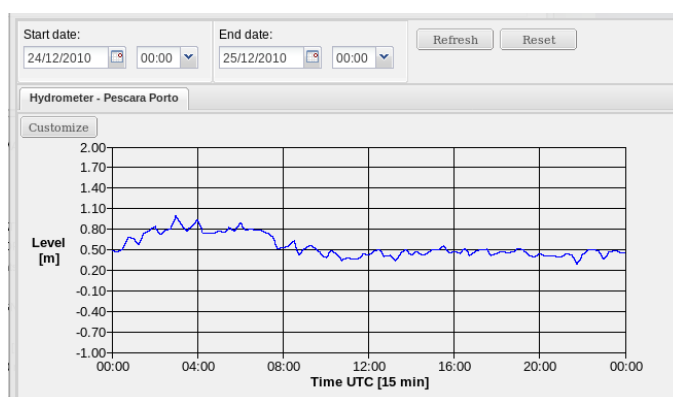


Figure 3.1.3: sea level hourly timeseries from 00UTC of 24th Dec 2010 to 00UTC of 25th Dec 2010, measured at the “Pescara Marina” station.

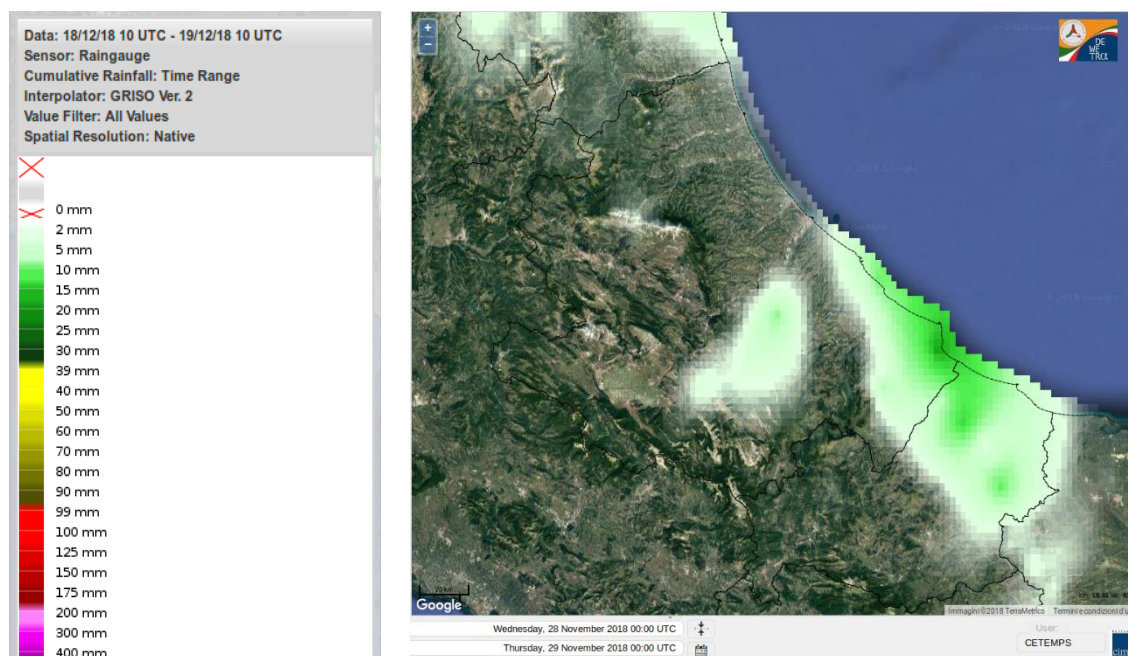


Figure 3.1.4: 24 h cumulated precipitation from 24th Dec 2010 00 UTC to 25th Dec 2010 00UTC over Abruzzo Region.

Hydrological simulations

In the simulation without the *waveheight* module activation, no warning state is given in the Pescara river mouth, as well as in all other grid-cells of the river final segment. The BDD index has the lowest values, as no increasing runoff rate is simulated, without consistent precipitation (fig. 3.1.5 - a). With the activation of the new parameterization, a moderate stress index is simulated in the river outlet, as indicated in the orange-coloured grid-cells (fig. 3.1.5-b). However, stress conditions are slightly underestimated, as the correction coefficient should be incremented, in order to give higher warning degree. Considering results obtained for other case studies, described in the following paragraphs, we preferred to maintain lower values of c , in order to avoid warning level overestimation, when storm surge is associated to precipitation, which is the most common situation.

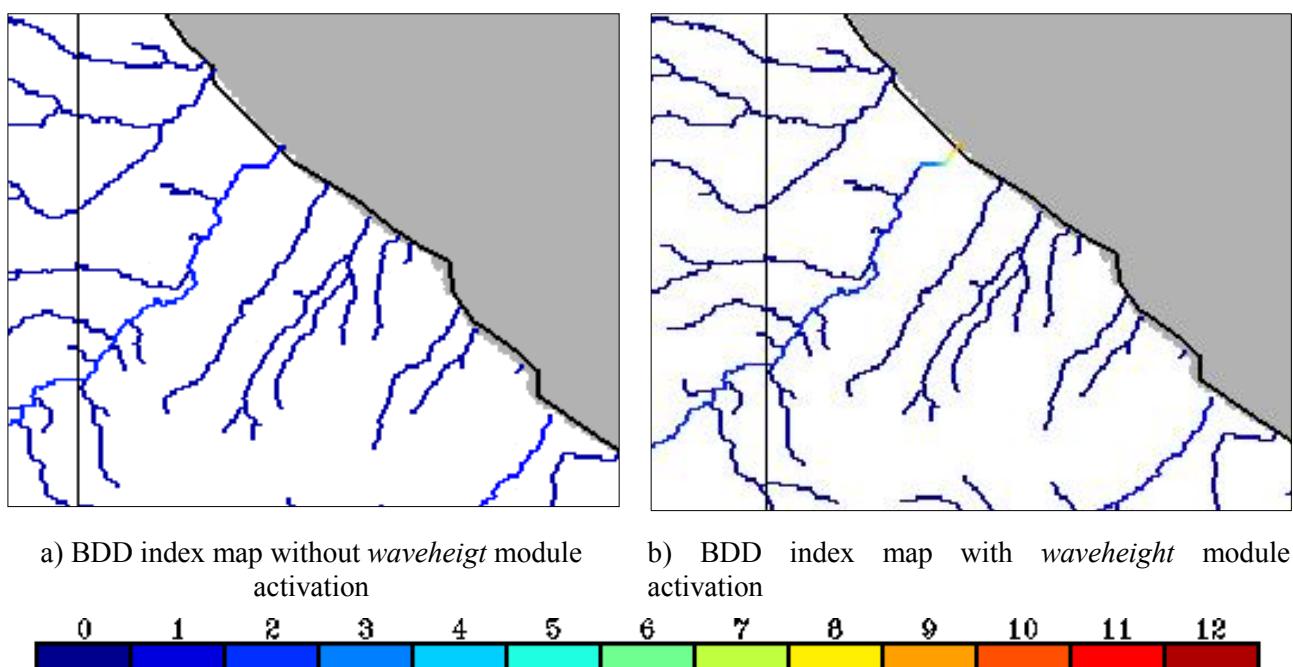


Figure 3.1.5: hydrological stress condition over the Pescara river basin represented by the BDD index (mm/h) on 24th December 2010. A comparison between the oldest version of CHyM and the AdriaMORE version for coastal flood monitoring.

3.2 Case study 15th November 2017

This case study was chosen, as its dynamics has been deeply investigated by the CETEMPS hydrological modeling group, for civil protection applications (Ferretti et al., 2019 and Lombardi et al., 2019). The event was one of the heaviest hydro-meteorological events to hit the Abruzzo region recently, being characterized by heavy precipitation and coastal storm at the same time.

Synoptic description

A deep intrusion of cold air from the arctic region turned in a cut-off low on the central Mediterranean region, during Nov 14th, 2017. This structure deepened and persisted over central

Italy from Nov 14th at 00UTC, till 16th Nov at 00UTC. During Nov 15th the low axis tilted, causing advection of northeastern flow over Abruzzo region and producing precipitation up to 200mm/24h (fig. 3.2.1).

Observations

In the morning of 15th November the Abruzzo Region was impacted by heavy rainfall, especially in the northern Adriatic area. The National Civil Protection Department (DPC) issued a meteorological alert over the region, due to the presence of “[...]local northeastern intense winds over the northern and central Adriatic area and along the central-northern Apennines ridge” (from the official meteorological warning bulletin issued on 15th Nov 2017, fig. 3.2.2).

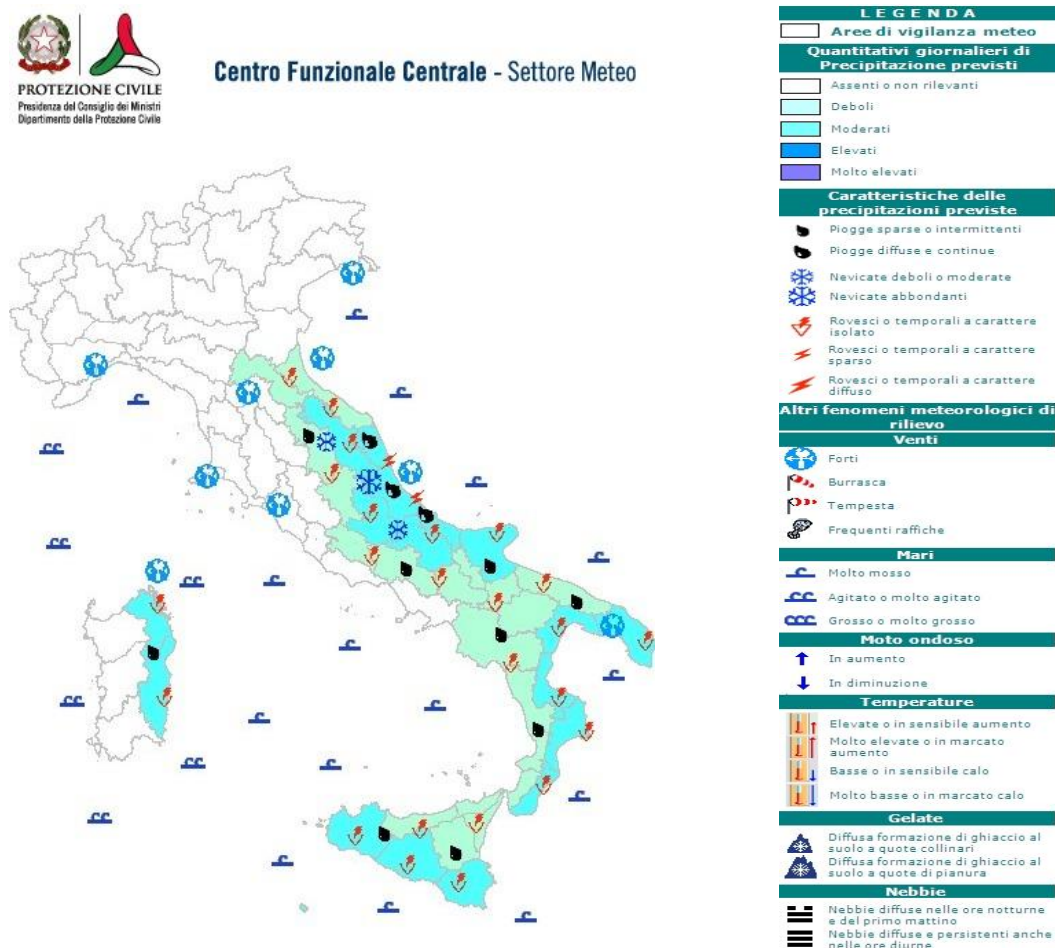


Figure 3.2.2: meteorological vigilance bulletin issued by the DPC on 15th Nov 2017.

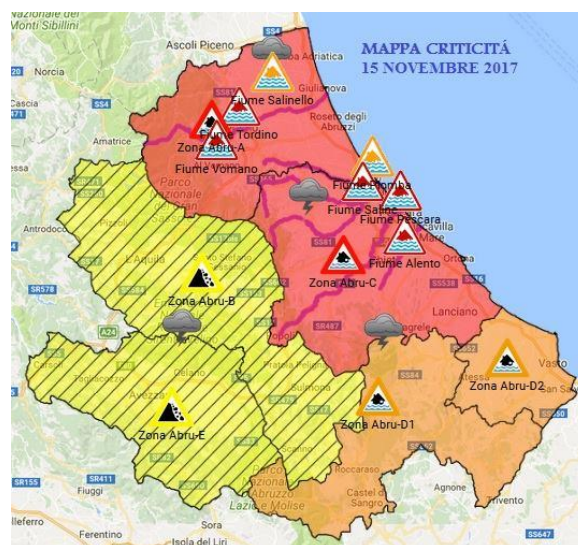


Figure 3.2.3: Hydrogeological Criticality Bulletin issued by the Civil Protection in the morning of 15 November 2017, where the Abruzzo region territory is divided into six warning areas (indicated with the prefix 'Zona Abru'), coloured according to the legend included. Triangle-shaped, thin-bounded signs are geolocated over relevant hydrometers and coloured according to the colour-code explained in table 1.7., resulting from observed data. Triangle-shaped, thick-bounded signs indicates the forecasted warning level in the reference warning area. Yellow triangle indicates landslide risk at warning area level, while, thunderstorm risk is assigned through figurative icon. Purple lines on the coastal warning areas highlight river segments where the red threshold has been overpassed.

Consequently, the Abruzzo Region Functional Centre (CFA) issued the hydrological and hydrogeological criticality bulletin, attributing the maximum warning level to the Pescara river basin (fig. 3.2.3).

As mentioned above, 24h cumulated rainfall was over 100 mm, with maximum peak of 200 mm over the Adriatic side (fig. 3.2.4). The prevalent wind direction is from North-East over the Apennines' chain, rotated from North-West along the coastal area (fig. 3.2.5). The discharge peak was registered in early afternoon of November 15th by the "Pescara S. Teresa Valle Diga" station: simultaneously, an increasing sea level in "Pescara Porto" sensor (fig. 3.2.6). The discharge peak and storm surge, occurring at the same times, caused a heavy, combined effect over the Pescara coastal area that was affected by severe flood, as reported by the official DPC press release. (<https://www.ilgiornaledellaprotezionecivile.it/index.html?pg=24>).

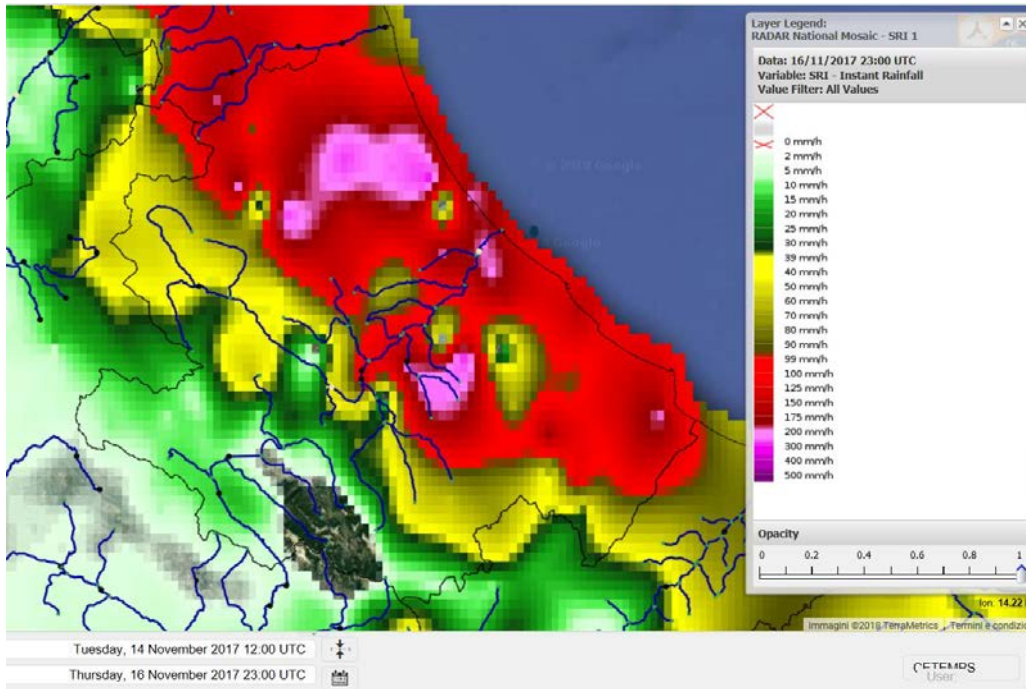


Figure 3.2.4: map of 24h accumulated precipitation from 15th Nov 00UTC to 16th Nov 00 UTC over the Abruzzo Region.

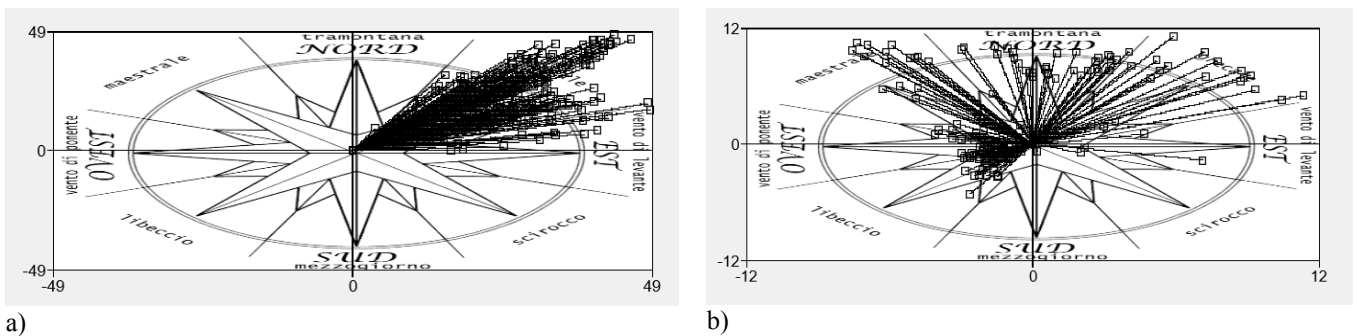


Figure 3.2.5: wind direction on 15th Nov 2017, overhead station “Campo Imperatore“ (a) and at ground level in Pescara Porto station (b).

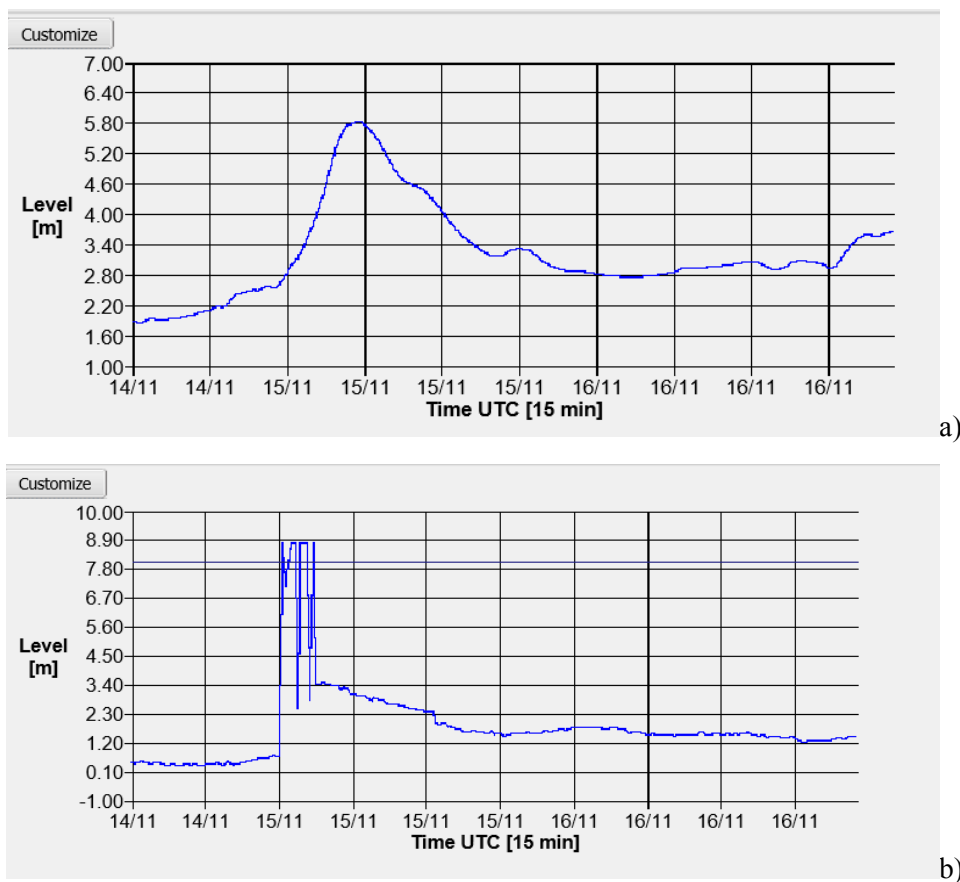


Figure 3.2.6: hydrometric level hourly timeseries at “Pescara S. Teresa Valle Diga” station (a) and sea level hourly timeseries at “Pescara Porto” station (b), measured during the event.

One of the main difficulties to assess coastal flood, is the lack of instrumental information in the last segment of a river channel. However, they can be inferred from Civil Protection and local authorities’ reports, as well as by using photographic documentation, as this is the case; in figure 3.2.7 an image of the Pescara canal port situation, taken by the firefighters is reported.



Figure 3.2.7: discharge peak in the Pescara canal port – 15th Nov 2017.

Hydrological simulations

In the simulation of this case study, as in the previous case, the CHyM model has been forced with rain gauge observed precipitation data, with a spin-up time of 5 days. Then, the BDD index has been calculated in the post-processing. The control simulation, set-up without using the *waveheight* module, the hydrological stress already has high values over the coastal areas, because of heavy precipitation occurrence. In the new simulation (fig. 3.2.8-a,b), the stress degree in the Pescara river mouth is higher, due to the added contribution of the storm surge.

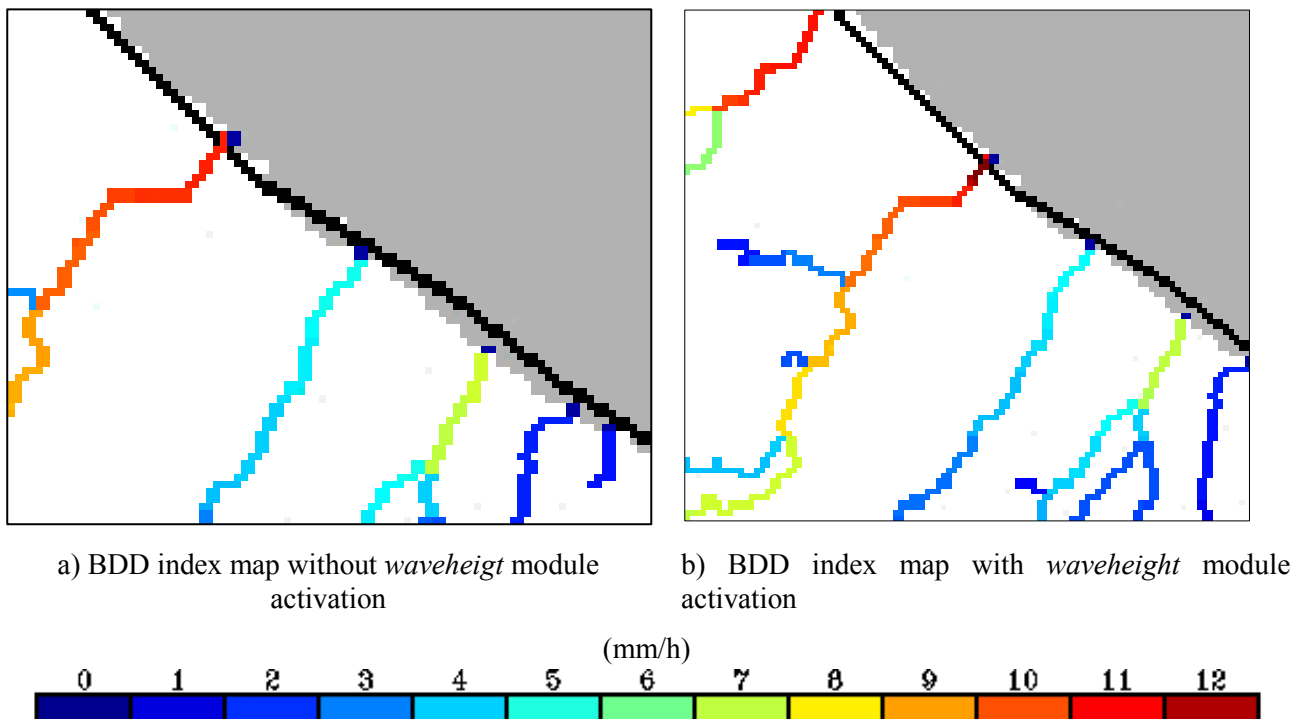


Figure 3.2.8: hydrological stress condition over the Pescara river basin represented by the BDD index (mm/h) on 15th November 2017. A comparison between the oldest version of CHyM and the AdriaMORE version for coastal flood monitoring.

3.3 Case study 28th November 2018

Synoptic description

The global circulation over Europe is reported in the map of geopotential field at 500 hPa, in figure 3.3.1. A deep through is descending from the Arctic toward the central Adriatic regions, where a minimum is located at ground level, causing cold air mass flow through the Balkans.

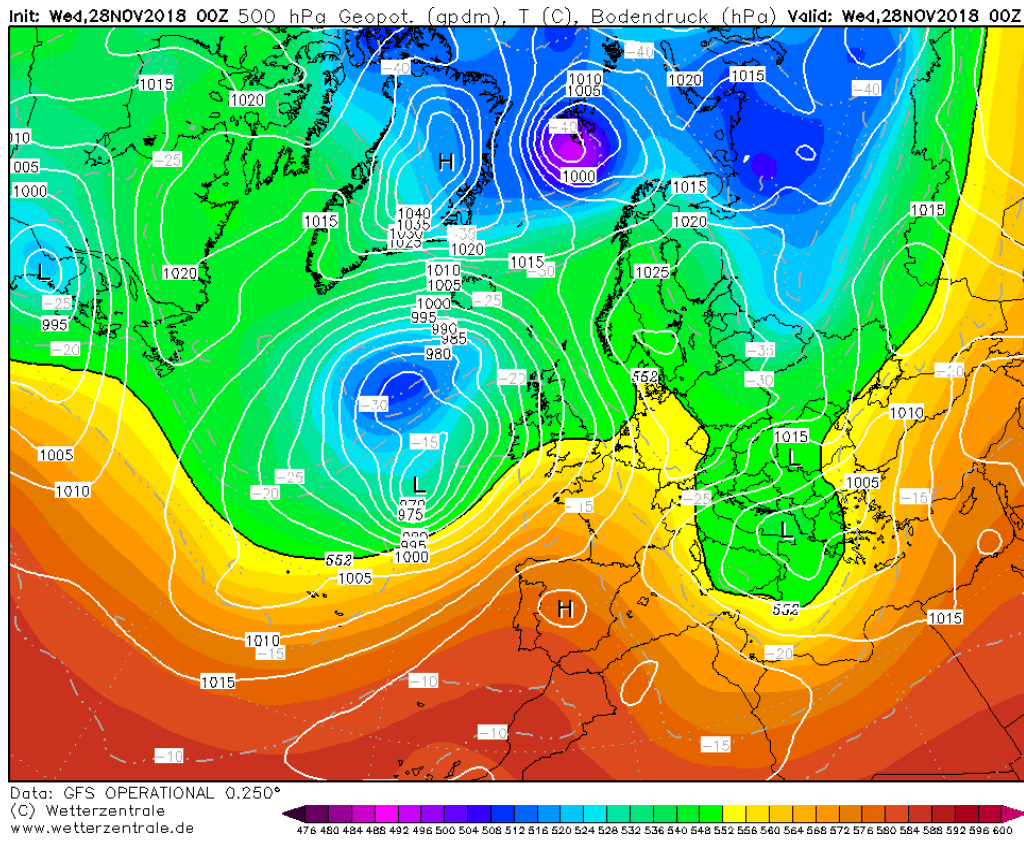


Figure 3.3.1: 500 hPa geopotential height over Europe on 28th Nov 2018 00UTC (colour shades) and pressure at ground level (isolines).

Observations

The meteorological surveillance bulletin issued by the DPC on 28th November 2018 (fig. 3.3.1) reported intense winds blowing over the Abruzzo coastal area. Floods were reported during the same morning over the Pescara littoral areas (fig. 3.3.2): such floods were not ascribable to heavy precipitation, as the total amount detected by the rain gauges network did not exceed 40 mm/48h, as reported in figure 3.3.3.



Figure 3.3.1: meteorological surveillance bulletin issued by the DPC on 28/11/2018.



Figure 3.3.2: storm surge over Pescara littoral area.

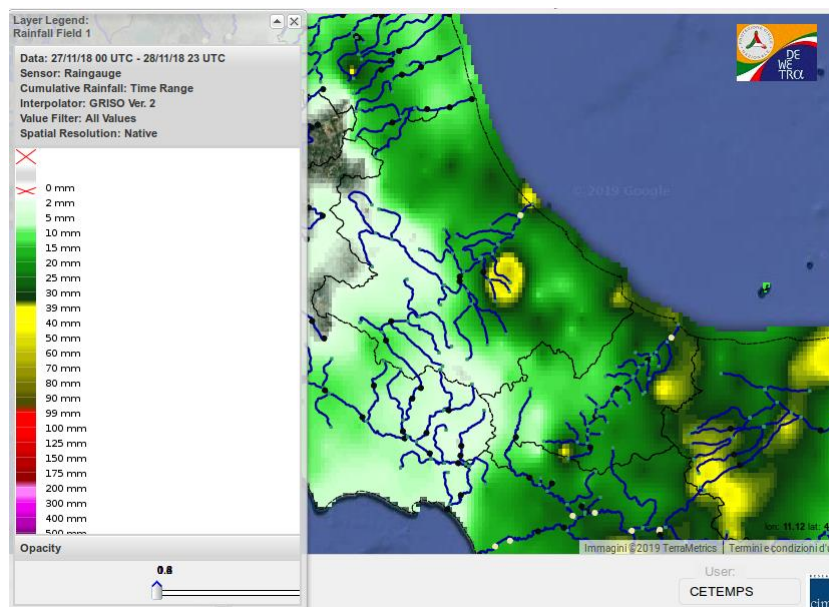


Figure 3.3.3: accumulated precipitation over Abruzzo from 27th Nov 2018 00 UTC to 29th Nov 2018 00 UTC.

As a consequence, floods occurred during this event were mainly driven by rising sea level (fig. 3.3.4)

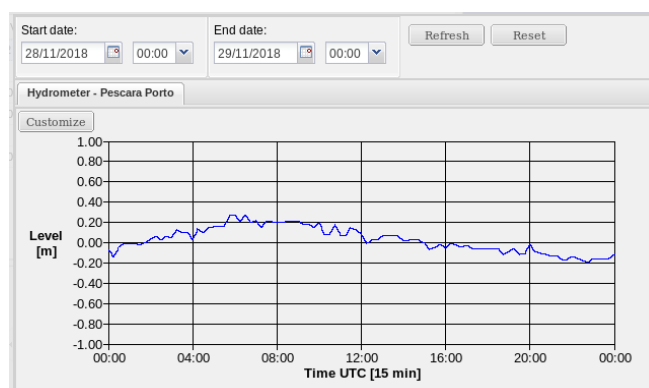


Figure 3.3.4: and sea level hourly timeseries at “Pescara Marina” station, measured during the event.

The BDD index resulting from the control simulation did not identify any warning level over the Pescara river outlet. The results from the activation of the *waveheight* module shows a negligible increment of the BDD index, as the storm surge mainly impacted the littoral areas, rather than river estuaries (fig. 3.3.5-a,b).

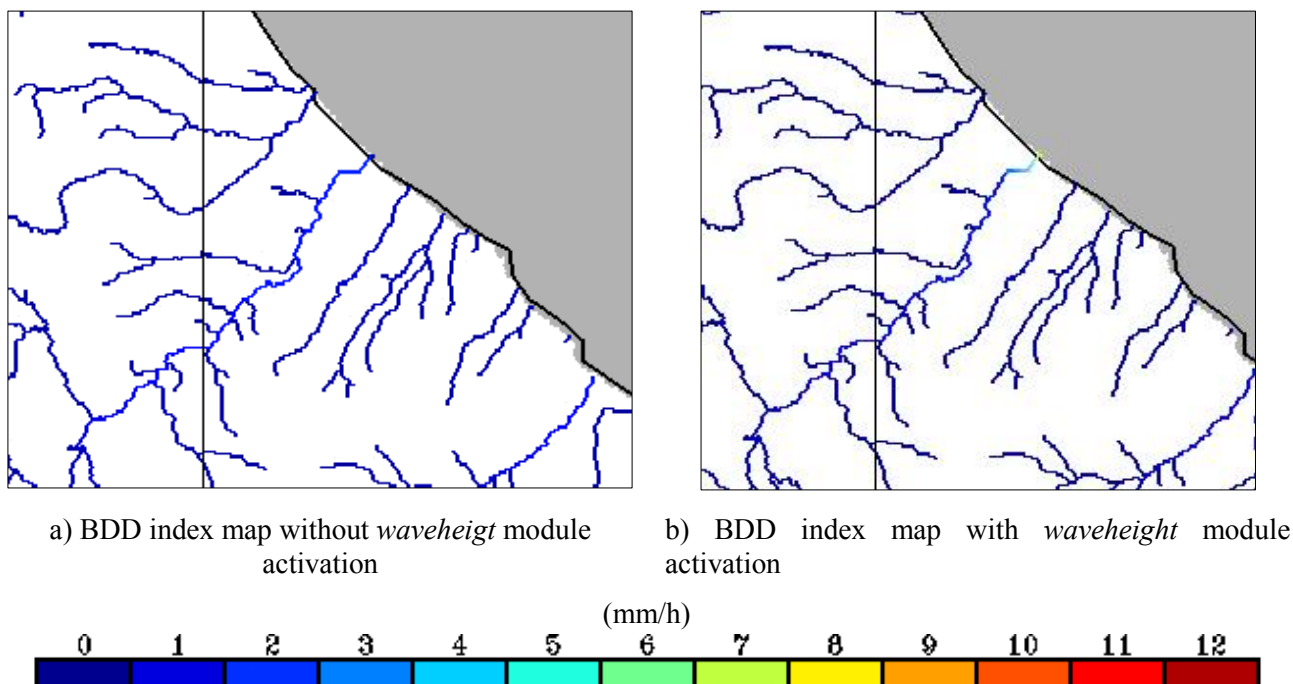


Figure 3.3.5: hydrological stress condition over the Pescara river basin represented by the BDD index (mm/h) on 28th November 2018. A comparison between the oldest version of CHyM and the AdriaMORE version for coastal flood monitoring.

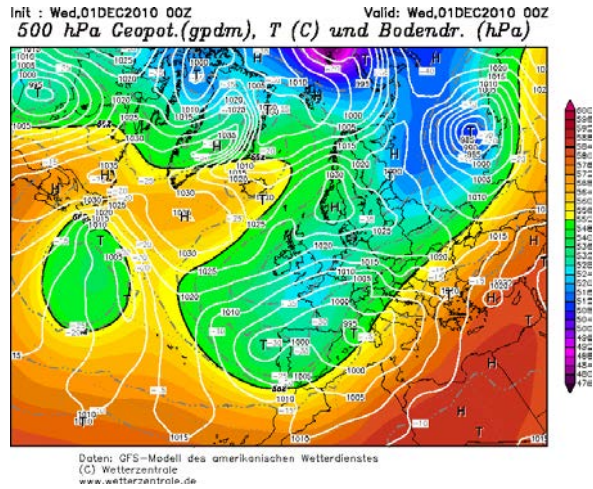
4. Neretva river

The case study on the Neretva basin has been agreed in collaboration with the Croatian Meteorological and Hydrological Service (DHMZ); it is characterized by both storm surge and heavy precipitation. Sea level data, as well as 24h accumulated precipitation from the rain gauges network has been provided: the latter, have been integrated with satellite rainfall estimation (3-hourly), in order to be coherent with the hydrological simulation temporal resolution. Moreover, information about the event dynamics, as well as synoptic description and observations, were provided by DHMZ.

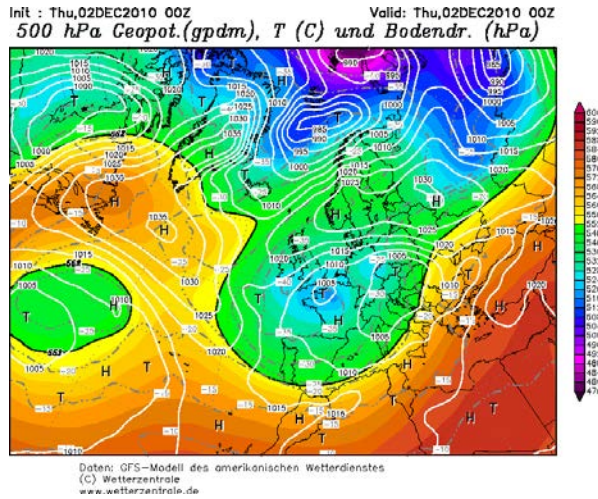
4.1 Case study 1st – 3rd December 2010

Synoptic description

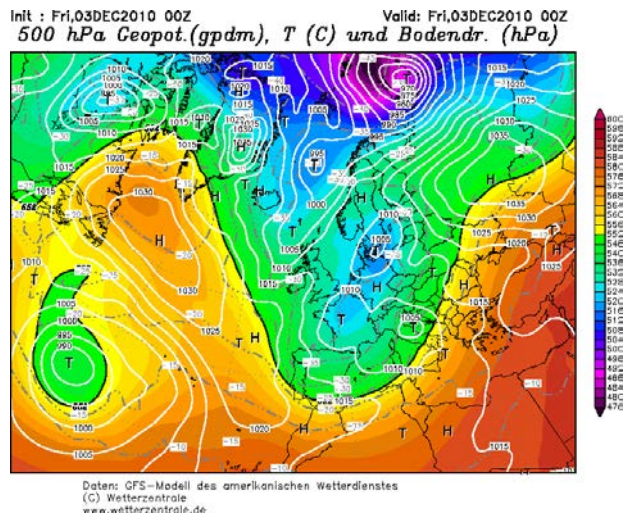
The synoptic situation over Europe was very complex on 1st December 2010 (fig. 4.1.1-a). A trough, originated from the Siberian latitudes, was extending to the western Mediterranean area with western tilting, causing moist advection from Southwest. The airmass flow was strengthened by a cyclogenesis over the Tyrrhenian Sea. The barometric pressure minimum at 500 hPa deepened during the following days; in the meanwhile, the barometric low at ground moved toward the Dalmatian coast (fig. 4.4.1-b,c).



a) geopotential height at 500 hPa (colour shades) and atmospheric pressure at ground level (isolines) at 1st Dec 2010 00UTC (from GFS Reanalysis)



b) geopotential height at 500 hPa (colour shades) and atmospheric pressure at ground level (isolines) at 2nd Dec 2010 00UTC (from GFS Reanalysis)

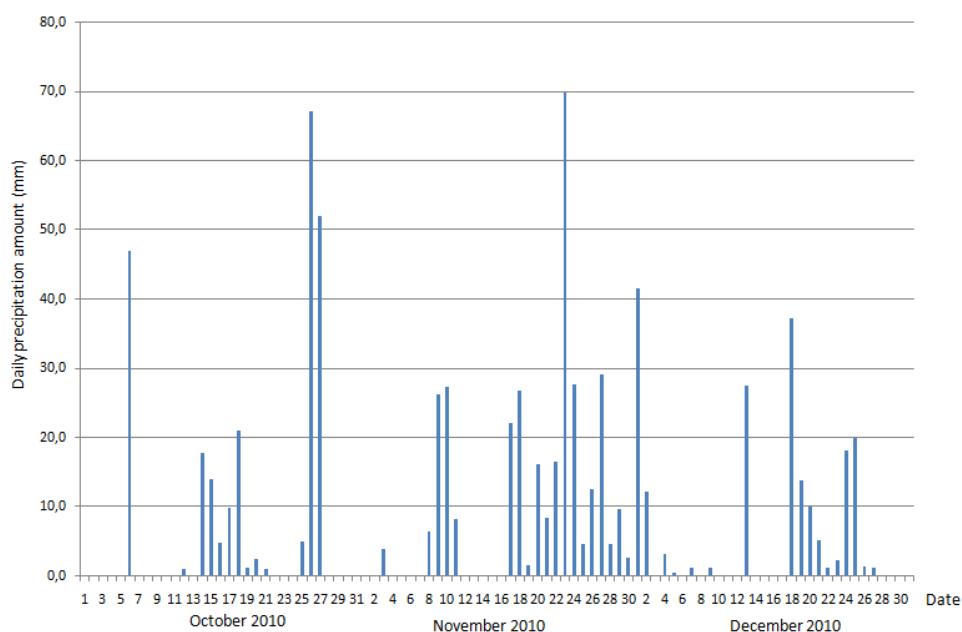


c) geopotential height at 500 hPa (colour shades) and atmospheric pressure at ground level (isolines) at 3rd Dec 2010 00UTC (from GFS Reanalysis)

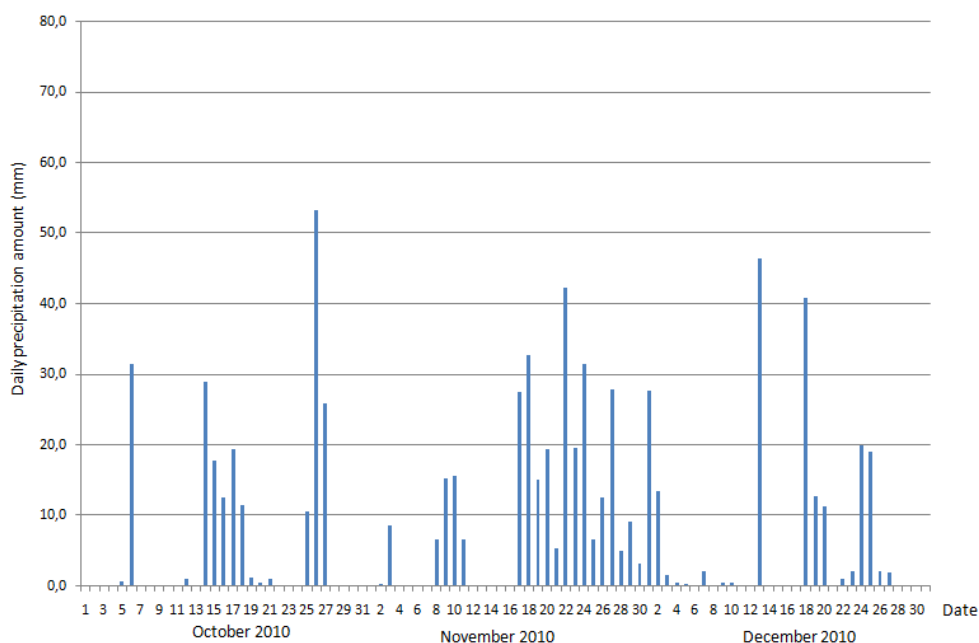
Figure 4.1.1: Synoptic situation during the event.

Observations

The case study analyzed in this section ends an exceptionally wet autumn, occurred in Croatia in 2010. Figure 4.1.2 shows the daily accumulated precipitation timeseries registered over the two rain-gauges installed in the Neretva basin terminal area. Constant, moderate to heavy precipitation occurred for many consecutive days, from 1st October 2010; as a consequence, a great impact on the analyzed event was exerted by the soil saturation, causing a decreasing infiltration rates and increasing surface runoff



a) daily precipitation registered in the Metkovic rain gauge.



b) daily precipitation registered in the Opuzen rain gauge.

Figure 4.1.2: October-December daily precipitation timeseries (from: DHMZ)

Discharge peaks occurring during the same period are reported, for the same hydrometric station, in figure 4.1.2. Maximum hydrometric level values during the event were 412 and 382 cm for Metkovic and Opuzen, respectively.

For the correction coefficient c , sea level data measured in the Ploce sensor were used (fig. 4.1.3).



Figure 4.1.3: sea level measured in the Ploce station (data from HHI – Hydrographic Institute of the Republic of Croatia)

As regards precipitation data to be used as input into the CHyM model, the daily rain gauges measurements have been integrated with satellite estimation 3-hourly/30 km maps, by using the GLDAS_NOA 0.25x0.25 deg database (Rodell et al., 2004), merged by using the cellular automata spatializing algorithm (Coppola et al., 2007).

The resulting rainfall field is shown in figure 4.1.4.

The hydrological stress maps obtained in the control simulation and new simulation using the *waveheight* module activation are shown in the next 4.1.5 figure. Maximum precipitation values occurred in 72 hours are around 80 mm, in this particular case study; such amount is not able to produce an significant peak discharge and appreciable stress index. The stress index is increased in the new simulation, however, if compared with the observed effects in the Neretva outlet surrounding areas (fig. 4.1.6), the yellow warning-level is still an underestimation. As a possible explanation, we think that the *waveheight* parameterization is not the responsible of such underestimation, that can be, more likely, caused by an underestimation of the soil moisture, due to limited spin-up time we set for operative run A climatological initialization of the hydrological simulation would benefit of an improvement of the soil moisture estimation and a better performance of the mode in this case..



Accumulated rain (mm)

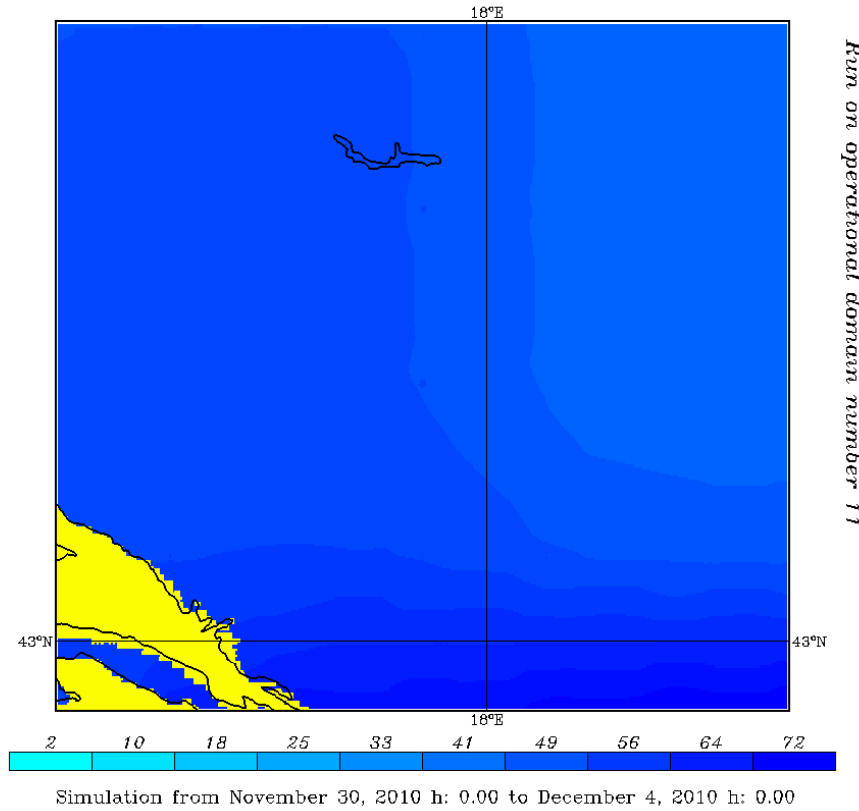


Figure 3.1.4: accumulated precipitation during the event (from 30th Nov 2010 00 UTC to 3rd Dec 2010 00).

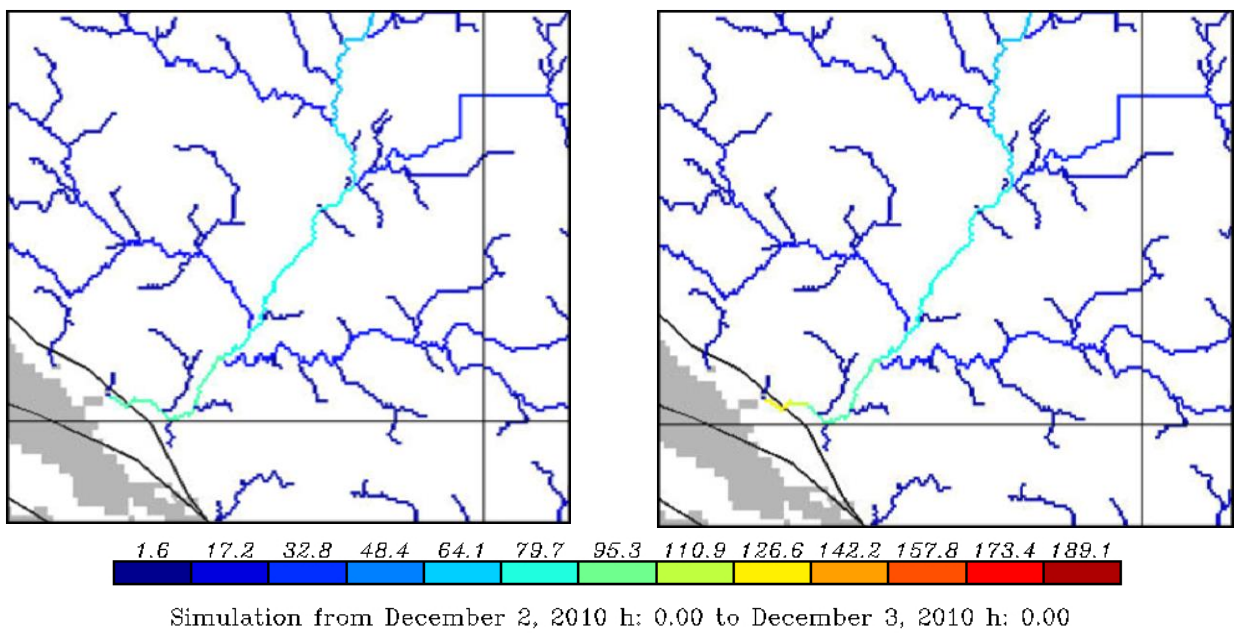


Figure 3.1.5: left panel: hydrological stress in control simulation; right panel: hydrological stress in new simulation.

References

- Bonacci, O. (2018); Hidrologija delte Neretve – Neretva Delta river Hydrology;
- Cowan W.L. (2012); “Estimating hydraulic roughness coefficients”, *Agr. Eng.*, 1956, 7, pp. 473-475;
- Coppola, E., Tomassetti B., Mariotti, L., Verdecchia, M. and Visconti, G. (2004); Cellular Automata algorithms for drainage network extraction and rainfall data assimilation, *Hydrol. Sci. J.*, **52(3)**, pp. 579-592;
- Coppola E., B. Tomassetti, L. Mariotti, M. Verdecchia, G. Visconti (2007), Cellular automata algorithms for drainage network extraction and rainfall data assimilation. *Hydrol Sci. J* **52(3)**: 579–92;
- Dorenbos, J. and W.O. Pruitt (1984 and 1992): Crop Water Requirements - Guidelines for Predicting Crop Water Requirements. - FAO Irrigation and Drainage Paper 24, FAO, Rome.
- Lighthill, M.J., G.B. Whitham (1955), On the kinematic wave II: a theory of traffic flow on the crowded roads. *Proceedings of The Royal Society of London, Series A*, 229 (317, 345);
- Ferretti, R., Lombardi, A., Tomassetti, B., Sangelantoni, L., Colaiuda, V., Mazzarella, V., Maiello, I., Verdecchia, M., and Redaelli, G. (2019): Regional ensemble forecast for early warning system over small Apennine catchments on Central Italy, *Hydrol. Earth Syst. Sci. Discuss.*, <https://doi.org/10.5194/hess-2019-223>, in review;
- Garzon J.L. and Ferreira C.M. (2016); “Storm surge modeling in large estuaries: sensitivity analyses to parameters and physical processes in the Chesapeake basin”, *J. Mar. Sci. Eng.*, **4**, 45, doi:10.3390/jmse4030045;
- Lombardi A., Tomassetti B., Colaiuda V. and Verdecchia M. (2018); “Flood alert forecast and mapping: test and validation of two hydrological stress indices over Italy”, Abstract, European Geoscience Union 2018, 9- 13 April 2018, Wien, Austria.
- Overtone, D. E. (1964), Mathematical refinement of an infiltration equation for watershed engineering. ARS41-99, Dept. Agriculture, Agriculture Research Service, U.S.D.A.;
- Packard NH, Wolfram S (1985) *J. Stat. Phys.*, **38**: 901–46;
- Passeri D., Hagen S., Smar D., Alimohammadi N., Risner A., e White R., (2011); “Sensitivity of an ADCIRC tide and storm surge model to Manning’s n.”, *Estuar. Coast., Model.* [Crossref];
- Pellicciotti F., B. Brock, U. Strasser, P. Burlando, M. Funk, J. Corripio (2005); An enhanced temperature-index Glacier melt model including the shortwave radiation balance: development and testing for Haut Glacier d’Arolla, Switzerland. *Journal of Glaciology*, **51**, No. 175;
- Rodell, M., Houser, P.R., Jambor, U., Gottschalck, J., Mitchell, K., Meng, C.-J., Arsenault, K., Cosgrove, B., Radakovich, J., Bosilovich, M., Entin, J.K., Walker, J.P., Lohmann, D. and Toll,

- D. (2004); The Global Land Data Assimilation System, (2004-01-01T00:00:00.000Z), doi:10.1175/BAMS-85-3-381, Data Author Publication;
- Sorooshian S., Hsu K.L., Coppola E., Tomassetti B., Verdecchia M., Visconti G. (Eds.) 2008 Hydrological Modelling and the Water Cycle Coupling the Atmospheric and Hydrological Models Series: Water Science and Technology Library Vol. **63**. ISBN: 978-3-540-77842-4.
- Singh, V.P.; Yu, F.X. (1990); “Derivation of Infiltration Equation Using Systems” Approach Journal of Irrigation and Drainage Engineering. Vol. 116, no. 6, pp. 837-858;
- Thornthwaite, C. W., and J. R. Mather (1957); Instructions and Tables for Computing Potential Evapotranspiration and the Water Balance. Publications in Climatology, Vol. 10, Laboratory of Climatology, Drexel Institute of Technology, 311 pp.;
- Tomassetti, B., E. Coppola, M. Verdecchia, G. Visconti (2005); Coupling a distributed grid based hydrological model and MM5 meteorological model for flooding alert mapping, Adv. in Geosci., vol. **2**, pp. 59-63, 2005.
- Todini E. (1996); The Arno rainfall-runoff model. Journal of Hydrology N. 175, 339-382;
- Verdecchia, M., E. Coppola, C. Faccani, R. Ferretti, A. Memmo, M. Montopoli, G. Rivolta, T. Paolucci, E. Picciotti, A. Santacasa, B. Tomassetti, G. Visconti, F. S. Marzano (2008); Flood forecast in complex orography coupling distributed hydrometeorological models and in-situ and remote sensing data. Meteorol. Atmos. Phys., **101**, 267–285;
- Wolfram, S. (1983); Statistical Mechanics of Cellular Automata. Rev. Mod. Phys. **55**, 601-644